

Paper No. 169f.

**Optical Investigation of the Interfacial Phenomena during Coalescence of  
two Condensing Drops and Shape Evolution of the Coalesced Drop**

*Shripad J. Gokhale, Sunando DasGupta, Joel L. Plawsky and Peter C. Wayner,  
Jr.*

*The Isermann Department of Chemical and Biological Engineering,*

*Rensselaer Polytechnic Institute, Troy, NY 12180-3590.*

Prepared for Presentation at

AICHE 2004 Annual Meeting, Austin, TX

November 8, 2004, Session Name: Poster Session: Interfacial Phenomena

## Abstract

Image analyzing interferometry is used to study the details of the shapes and coalescence of condensing drops of 2-propanol on a quartz surface. The measured thickness profiles give fundamental insights into the transport processes within the drop and its evolution from asymmetric to symmetric shape. The results show the presence of a thin flat film adjacent to the condensing drops and the adsorbed film thickness is found to be constant and independent of the point of measurement. We found that in addition to the apparent contact angle, the determination of the profiles of the local interfacial tangent, curvature and curvature gradient enhances the description of the growth and coalescence of the drops. We observed that the drops coalesce and there is a liquid flow from the smaller drop towards the bigger drop due to the difference in their shape dependent pressure fields. This was also shown by the calculations of the center of mass of the two coalescing drops and that of the coalesced drop. The curvature and its gradient describe the process more completely than the contact angle, unless we pick the contact angle at the inflection point. The asymmetric coalesced drop self-adjusts and evolves into a symmetric shape due to the capillary flow within the drop. The calculated pressure field in the coalesced, asymmetric drop is consistent with the required capillary assisted flow from the receding to the stationary front of the asymmetric drop, till it becomes symmetric. The calculations of the average shear stress, the decrease in the interfacial excess energy, interfacial pressure field, and the positions of the center of mass give a physical understanding of the spreading and coalescence of the drops.

## Observations and Results

Naturally occurring interference fringes result due to the reflection of the monochromatic light ( $\lambda=543.5\text{nm}$ ) at the liquid-vapor and liquid-solid interfaces (Zheng et al., 2002). Recorded images of the interference fringes for the condensing drops were analyzed to get the profiles of the thickness, slope (a measure of the apparent contact angle), and the curvature at each pixel location ( $0.177\mu\text{m}$ ) along the drop using an image analyzing technique based on the reflectivity measurement (Gokhale et al., 2004a).

Experimentally obtained optical micrographs of the condensing drops during the coalescence process are shown in Fig. 1. Figures 1(a) and 1(b) show that the two drops grow in size due to condensation and approach each other, still keeping their symmetric shape intact. Figure 1(c) depicts the merging of the two drops resulting in an elongated asymmetric drop. The drop shape evolves and eventually becomes symmetric [Fig. 1(d)].

The spreading velocities of the larger and the smaller drops before coalescence are  $0.14\text{ m/s}$  and  $0.12\text{ m/s}$  respectively. Assuming that the drops have a spherical cap shape before coalescence, Eq. (1) shows that the surface heat flux ( $q''_{\text{surface}}$ ) is proportional to the rate of change of the radius of the drop.

$$q''_{surface} \propto \frac{\text{volume change rate}}{\text{surface area}} = \frac{2\rho R^2 \left( \frac{dR}{dt} \right)}{2\rho R^2} = \frac{dR}{dt} \quad (1)$$

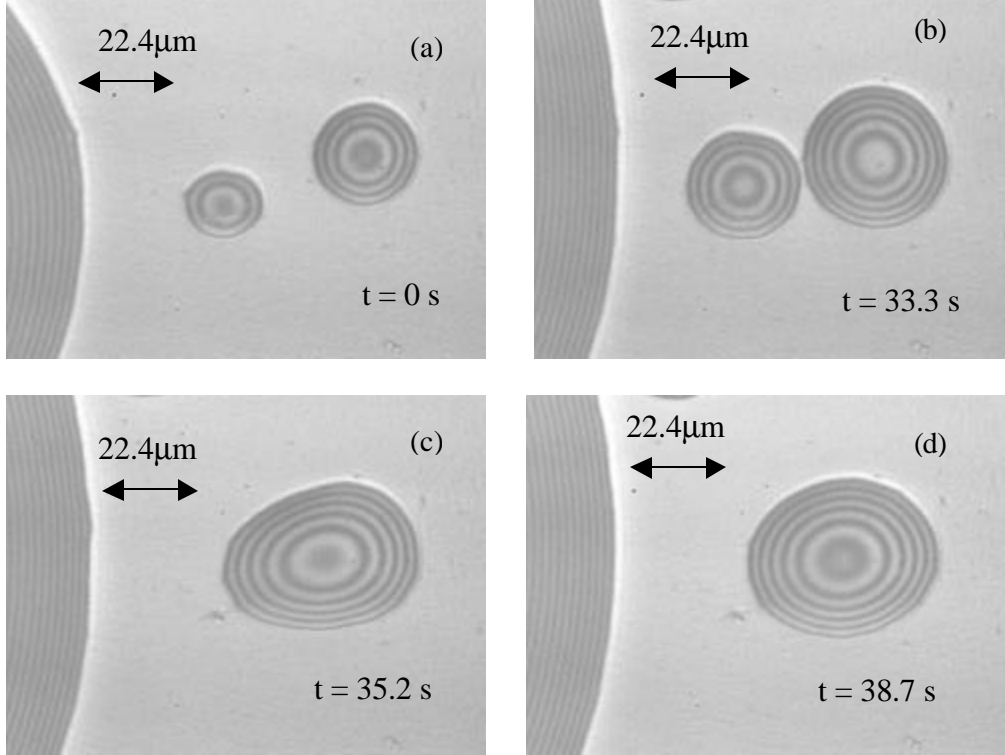


**FIG. 1(a-d). Optical micrographs of the condensing drops during the coalescence process as a function of time.**

Hence, the surface heat flux for the larger drop is larger compared to the smaller drop. The difference between the surface heat fluxes of the smaller and the larger drops is related to the differences in their contact angles and curvatures. The experimentally measured thickness profiles of the two drops [shown in Fig. 1(b)] before merging are shown in Fig. 2 (a). The profiles are similar on all the sides of the individual drops, as the drops spread symmetrically before merging. There is a thin flat film adsorbed between the condensing drops. The measured value of the adsorbed film thickness is  $\delta_0 = 5.4 \pm 1 \text{ nm}$  and is found to be the same for both the drops. It remains constant as the drops grow and spread during condensation. The corresponding slope angle profiles (a measure of the slope of the profile) are shown in Fig. 2(b). The slope angle of the liquid-vapor interface continuously changes as the interface merges with the thin adsorbed flat film on the surface. It was found that a higher contact angle gives a higher spreading velocity.

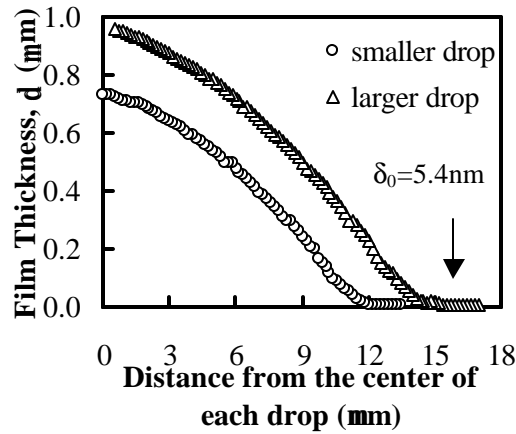


**FIG. 2 (a).** Film thickness profiles of the condensing drops [shown in Fig. 1(b)] before coalescence.

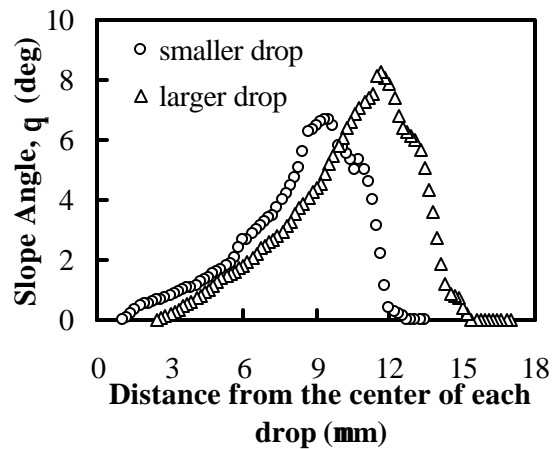


**FIG. 2 (b).** Slope angle profiles of the condensing drops [shown in Fig. 1(b)] before coalescence.

The curvature profiles calculated using the experimental data for the two drops are shown in Fig. 2(c). As the magnitude of the negative curvature at the apex of the smaller drop is more than that of the larger drop, the increase in the interfacial vapor pressure is more for the smaller drop. Thus, the rate of condensation of the larger drop is more than that of the smaller drop. Thus, the experimental technique correctly captures the effect of curvature on surface heat flux and shows the presence of a curvature gradient (pressure gradient) for flow within the condensing drops.

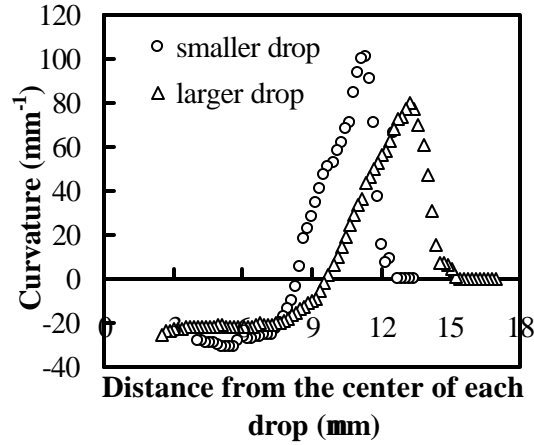


**FIG. 2 (c). Curvature profiles of the condensing drops [shown in Fig. 1(b)] before coalescence.**

The instant the two drops touch each other, the smaller drop merges into the larger drop because of the difference in their pressure fields and the resultant drop is asymmetric on its two sides as shown in Fig. 1(c). We note the higher pressure inside the smaller drop at the apex.

The curvature profiles of the coalesced asymmetric drop are plotted in Fig. 3.

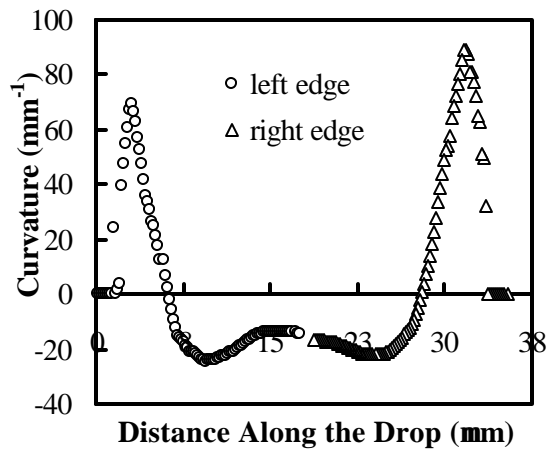


**FIG. 3. Curvature profiles of the initially asymmetric coalesced drop [shown in Fig. 1(c)] on two sides.**

From Fig. (3), we see that the curvature at  $\delta=0.098\mu\text{m}$  and in the contact line region (the inflection point) is lower on the receding front of the drop than that on the stationary front. The curvature profiles represent the capillary pressure within the liquid drop as modeled by the augmented Young-Laplace equation [e.g., Gokhale et al. 2003, Potash and Wayner 1972, DasGupta et al. 1994]. The

difference between the capillary pressures on the receding and the stationary fronts of the coalesced asymmetric drop is the driving force for the shape evolution towards a symmetric shape (Gokhale et al., 2004b). The measured interfacial force per unit interline length of the control volume (F) between the drops is given by Eq. (2).

$$F = \sigma_{lv} (\cos \theta_2 - \cos \theta_1) + \sigma_{lv} d(K_2 - K_1) \quad (2)$$

Here, the subscripts 1 and 2 represent the smaller and the larger drop respectively,  $\sigma_{lv}$  is the surface tension of the liquid ( $\sigma_{lv}=20.93 \times 10^{-3} \text{ J/m}^2$ ),  $\theta$  is the apparent contact angle. The thickness  $\delta$  is the thickness of the film at the ends of the control volume where  $K$  and  $\theta$  are measured at the same values of  $\delta=\delta_1=\delta_2$ . At  $\delta=0.098 \mu\text{m}$ , where disjoining pressure is negligible, we get  $F=1.2769 \times 10^{-5} \text{ N/m}$  just before the drops coalesce [for the drops shown in Fig. 1(b)]. The driving force is directed from the smaller drop towards the larger drop and it is positive for the experimental data of the apparent contact angles and the curvatures of the two drops. This shows the decrease in the interfacial free energy (per unit area) causing the merger of the smaller drop towards the larger drop.

The coalesced drop evolves into a symmetric shape [Fig. 1(d)] due to the curvature gradient and the resulting capillary flow within the drop as the left side of the coalesced drop recedes towards the right front. The lower (positive) value of the concave curvature [shown in Fig. 3] near the contact line region of the receding front of the drop signifies a higher liquid pressure ( $P_l$ ) compared to the stationary front based on the augmented Young-Laplace equation, Eq. (3).

$$P_v - P_l = K\sigma_{lv} - \frac{A}{6\pi d^3} \quad (3)$$

Where,  $P_v$  is the vapor pressure,  $P_l$  is the pressure inside the liquid,  $K$  is the curvature of the liquid-vapor interface,  $\sigma_{lv}$  is the surface tension, and  $\delta$  is the film thickness of the liquid. The second term on the right hand side of the equation signifies the van der Waals interactions. The symbol  $A$  is the Hamaker constant. The van der Waals interactions are long range interactions and are significant till  $\delta \cong 100 \text{ nm}$ . Thus, there is a capillary flow of the liquid from the receding front to the stationary front within the coalesced drop. As the shape of the drop evolves toward a symmetric shape, the difference in the liquid pressures, which causes the shape evolution, decreases. Thus, the driving force for the liquid flow from the receding front toward the stationary front decreases as the asymmetry in the shape of the coalesced drop decreases. Ultimately the liquid pressures on both the sides of the coalesced drop become equal when the coalesced drop evolves into a symmetric shape. This is demonstrated from the curvature profiles of the symmetric drop after shape evolution in Fig. 4. Thus, the evaluated pressure field is consistent with the shape evolution of the coalesced drop.

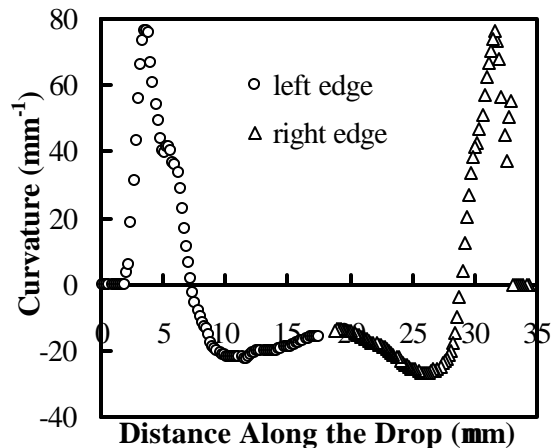


**FIG. 4. Curvature profiles of the symmetric coalesced drop [shown in Fig. 1(d)] on two sides.**

### Acknowledgement

This material is based on the work supported by the National Aeronautics and Space Administration under grant # NAG3-2383. Any opinions, findings and conclusions expressed in the paper are those of the authors and do not necessarily reflect the view of NASA.

### References

- Zheng, L., Y. -X. Wang, J. L. Plawsky, and P. C. Wayner, Jr., "Effect of Curvature, Contact Angle, and Interfacial Subcooling on Contact Line Spreading in a Microdrop in Dropwise Condensation," *Langmuir*, **18**, 5170 (2002).
- Gokhale, S. J., Plawsky, J. L., Wayner P. C. Jr., DasGupta, S., "Inferred Pressure Gradient and Fluid Flow in a Condensing Sessile Droplet Based on the Measured Thickness Profile", *Phys. Fluids* **16**, 1942 (2004a).
- Gokhale, S. J., Plawsky, J. L., Wayner, P. C. Jr., "Experimental Investigation of Contact Angle, Curvature and Contact Line Motion In Dropwise Condensation and Evaporation," *J. Colloid Interface Sci.* **259**, 354 (2003).
- Gokhale, S. J., DasGupta, S., Plawsky, J. L., Wayner P. C. Jr., "Reflectivity Based Evaluation of the Coalescence of Two Condensing Drops and Shape Evolution of the Coalesced Drop", *Phys. Rev. E* (Accepted, In Press 2004b).
- Potash, M. Jr. and Wayner, P. C. Jr., "Evaporation From a Two-Dimensional Extended Meniscus," *Int. J. Heat Mass Transfer*, **15**, 1851 (1972).
- DasGupta, S., I. Y. Kim, and P. C. Wayner, Jr., "Use of the Kelvin-Clapeyron Equation to Model an Evaporating Curved Microfilm," *J. Heat Transfer*, **116**, 1007 (1994).